First terrestrial occurrence of the complex phosphate chladniite: Crystal structure refinement by synchrotron through-the-substrate microdiffraction

ORIOL VALLCORBA[1], LLUÍS CASAS[2], FERNANDO COLOMBO[3*], CARLOS FRONTERA[3] and JORDI RIUS[3]

[1] ALBA Synchrotron Light Source, Cerdanyola del Vallès, Barcelona, 08920, Spain

[2] Unitat de Cristal·lografia i Mineralogia, Dpt. de Geologia, Universitat Autònoma de Barcelona, Bellaterra, Catalonia, 08193, Spain

[3] Institut de Ciència de Materials de Barcelona, CSIC, Campus de la UAB, Bellaterra, Catalonia, 08193, Spain

Corresponding author, e-mail: jordi.rius@icmab.es

Abstract: Chladniite, a complex phosphate species belonging to the fillowite group so far only found in meteorites, was identified in a pegmatite from Córdoba (Argentina) as inclusions in beusite. Applying synchrotron through-the-substrate microdiffraction technique (tts-μXRD) to polished thin sections prepared on very thin glass substrates (0.1 mm), diffraction data with nearly single-crystal quality were directly measured at selected chladniite microvolumes of the section. Chladniite is trigonal (space group *R*-3), with a = 15.0133(3) Å, c = 42.887(2) Å, V = 8371.6(5) Å^3. The subsequent crystal structure refinement confirms that the accuracy attainable by using 0.1 mm thick glass-substrates is comparable to that of routine single-crystal measurements [R_1=3.34% for 1617 unique reflections]. The refined crystal structure of pegmatitic chladniite differs from meteoritic one in the cation ordering (Mg, Fe+Mn and Ca) at the various metal sites, with Mn being dominant at the M(1) position

Key-words: tts-μXRD; chladniite; complex phosphates; fillowite group; polished thin section; synchrotron radiation; meteorites; pegmatites; thin glass substrates; crystal structure refinement

*Current address: CICTERRA-UNC, CONICET, FCEFyN, Vélez Sarsfield 1611 (X5016GCA) Córdoba, Argentina

1. Introduction

The synchrotron through-the substrate microdiffraction (tts-μXRD) technique consists of obtaining synchrotron diffraction data from a sample mounted in a thin section of the type routinely used for petrographic studies (Rius *et al.*, 2011). The small beam diameter (about 15 μm) allows collection of data (measured in transmission mode) from single crystals without the need of removing them from the thin section, thus preserving the textural context and avoiding a possible sample deterioration during extraction of a fragment. A complete description of the technique is provided by Rius *et al.* (2015). As the method development evolved, it became evident that incoherent scattering from the glass substrate was one of the most limiting factors, as it tended to obscure weak reflections and also restricted the maximum rotation angles that could be reached during data collection. To overcome this problem, we present here an alternative way of sample preparation and test it by refining one of the most complex phosphate structures belonging to the fillowite group. Since the preparation of thin sections on very thin glass-substrates is of potential interest for mineralogists and petrologists, a short description of this simple preparation technique is also given.

The fillowite group

Fillowite was first described as a new mineral species by Brush and Dana (1879), who considered it as monoclinic (pseudo-trigonal) on the basis of morphological observations. That the symmetry is trigonal and that the true space group is *R*-3 was later reported by Fisher (1965). However, sixteen years were still necessary until the first crystal structure determination was published (Araki and Moore, 1981). Fillowite group minerals have one of the most complex phosphate structures known to date. Although fillowite crystallizes in space group *R*-3, there are 45 independent atom positions, with $a \approx 15.3$, $c \approx 43.3$ Å, and $Z = 18$. Subsequent structural refinements of related minerals have shown variable order in the ten metal sites, some of them being occupied by a single cation but mostly by Mg and (Fe+Mn) in different ratios. The coordination number of these sites is variable, ranging from 5 (distorted trigonal bipyramids) to 6 (octahedral). The provisional classification scheme suggested by Grew *et al.* (2006) where these ten M sites are grouped together for the purpose of species definition seems advisable in order to avoid a proliferation of names. According to this proposal the generalized formula for members of the fillowite group is $(Na,K,\square)_2(Na,K)_6(M^{2+},Na,K)_8(M^{2+},Y,REE,Na)(M^{2+},M^{3+})_{43}(PO_4)_{36}\cdot nH_2O$ with □ denoting a vacancy. Several isotypic compounds, some of them including elements not found in natural samples, such as Cd and Sc, have been synthesized (e.g. Antenucci *et al.*, 1996, Hatert and

Fransolet, 2003). Some of these compounds, such as that reported by Jerbi *et al.* (2010), show additional crystallographic sites not yet described for natural members of this group. Charge balance by substitution among M^{3+}, M^{2+} and M^{+}, coupled with vacancies, affords a flexible way of accommodating varying ratios of metals with different oxidation states. An example are the synthetic compounds $Ca\square_2Na_6(Ca_6Na_2)CaMg_{42}(PO_4)_{36}$ (Domanskii *et al.*, 1982), and $CaNa_2Na_6(Ca_4Na_4)Ca(Ca_6Cd_{12}Mg_{24})_{\Sigma 42}(PO_4)_{36}$ (Antenucci *et al.*, 1996). In natural samples, trivalent metals are very minor, except for stornesite-(Y), where Y^{3+} is an essential structural component ordered at the M(1) site. Potassium is also usually very low (up to 0.34 wt.% K_2O in fillowite from the Animikie Red Ace pegmatite, USA, Fransolet *et al.* 1998), but it becomes dominant in a (presumably) K analogue of galileiite found in a meteorite (Olsen *et al.*, 1999). Regarding the H_2O content, in most cases $n = 0$, but one synthetic phase studied by Keller *et al.* (2006) is of particular interest, as it contains a small amount of molecular H_2O ($n = 0.5$). A number of analyses of fillowite group minerals report H_2O (see Keller *et al.*, 2006 for a review), but the accuracy of these values has been questioned and the role of H_2O, if any, has yet to be established in natural phases. The chemical compositions of fillowite group minerals, as well as those of minerals which likely belong to this group but whose crystal structure has not been solved, are summarized in Table 1. Xenophyllite, $Na_4Fe^{2+}{}_7(PO_4)_6$, space group *P*-1 (IMA 2006-006), has been described as belonging to the fillowite group. However, a definitive classification will have to wait until more information becomes available.

Table 1

Chladniite, the Ca and Mg end-member of the fillowite group, was discovered in the Carlton IIICD iron meteorite (McCoy *et al.*, 1994). Steele (1994) used a fragment drilled out of a polished thin section for solving its crystal structure. Subsequently, this phosphate was found in another meteorite (Floss, 1999). Note that, depending on the classification scheme adopted, the synthetic phosphates described by Domanskii *et al.* (1982) and Hatert and Fransolet (2003) may also be considered chladniite. However, they present a different stoichiometry, i.e., $Ca_2Na_6(Ca_6Na_2)CaMg_{42}(PO_4)_{36}$ (Domanskii *et al.*, 1982) vs. $CaNa_2Na_6(Ca_4Na_4)Mg_{43}(PO_4)_{36}$ (McCoy *et al.*, 1994) vs. $CaNa_2Na_6(Ca_4Na_4)Ca_7Mn_{12}Mg_{24}(PO_4)_{36}$ (Hatert and Fransolet, 2003). In any case, the first terrestrial finding of chladniite is the one reported in the present contribution (Fig. 1). The sample comes from the Tablada I pegmatite, in Pocho Department, Córdoba Province (central Argentina). Its geological setting was described by Colombo *et al.* (2012), where the material was provisionally identified as maghagendorfite based on compositional data acquired with an electron microprobe.

Fig. 1 shows the photomicrograph of the polished thin section of the sample which also contains beusite, garnet and a still unidentified phase.

Figure 1

2. Experimental

2.1. Chemical analyses of chladniite

The sample was studied in three different labs in Madrid, Córdoba (Argentina) and Barcelona using BSE imagery and quantitative electron microprobe analysis. The analyses reported here were obtained with a JEOL 8900 electron microprobe (by wavelength-dispersive spectroscopy), located at the Centro de Microscopía Electrónica Luis Brú (Universidad Complutense de Madrid). Operating conditions were: 15 kV, 20 nA, and a beam diameter of 2-5 μm. Standards were kaersutite (Ca,Mg), fluorapatite (P), almandine (Fe,Mn), gahnite (Zn) and albite (Na). Other elements specifically sought but found to be below the detection limits (in ppm) were Al (260), Si (400), Ti (440), Cu (620), Cl (240) and Sr (900). No additional elements with Z above 6 (carbon) were detected in EDS spectra. The average chemical composition (in wt.%) is P_2O_5 45.29, FeO 17.37, MnO 14.42, MgO 11.56, CaO 5.52, ZnO 0.37, Na_2O 5.62, total 100.15. The atomic proportions, scaled to 108 P atoms per formula unit (*apfu*) for direct comparison with the results of the structural analysis (and with O for charge balance), are $Na_{30.69}Ca_{16.66}Mg_{48.56}Mn_{34.41}Fe_{40.92}Zn_{0.77}P_{108}O_{426.67}$.

2.2 Preparation of polished thin sections on 0.1 mm glass-substrates

To diminish the scattered background in the tts-μXRD experiment it is most convenient to reduce the thickness of the glass substrate of the polished thin section. However, risk of fracture also increases with decreasing thickness. To reduce the thickness from the usual 1 - 1.5 mm to 0.1 mm, a two-stage method was developed (Fig. 2). The first stage of the method consists of gluing two glasses together with an acetone-soluble adhesive. These glasses are a standard slide (about 1.5 mm thick) and a cover slide (about 0.1 mm thick). The resulting composite glass is then handled following the classical thin-section preparation procedure: *i*. the rock slice is glued with epoxy to the cover slide; *ii*. the rock sample is thinned to the desired thickness; *iii*. the thin section is finished with a mirror polish for electron microprobe analysis. The thin section in this form can be safely manipulated. It can also be studied using polarized light microscopy, and areas of interest are selected by drawing a circle with a fine-point permanent marker. After carbon coating, minerals are

examined with electron microscopy (which may reveal chemical zoning not evident in polarized light microscopy), and interesting points are quantitatively analyzed by electron microprobe. The second stage of the method begins once all relevant chemical information and images have been obtained. The thin section is allowed to soak in solvent for *ca*. 24 hours. This process dissolves the adhesive between the two glass slides (but not between the rock and the glass immediately beneath it), and the rock-plus-cover assemblage can be cleanly separated from the thick glass (standard slide), so that the sample is already finished for the tts-μXRD experiment. An additional benefit of the procedure is that the solvent also dissolves the permanent ink around the areas of interest. Since the carbon coating was applied on top of the ink, the now-gone circles are still visible as pale lines on a darker background (caused by the carbon still adhered to the rock surface). This helps to identify and hence to locate the selected areas in the diffraction experiment. As can be seen in Fig. 3, the 0.1 mm-thick glass substrate produces a very low background.

Figure 2

Figure 3

2.3 Synchrotron tts-μXRD data collection

The tts-μXRD experiment was performed at the microdiffraction/high pressure station of the MSPD beamline (ALBA Synchrotron) (Fauth *et al.*, 2013). This endstation is equipped with Kirkpatrick-Baez mirrors providing a monochromatic focused beam of 15 x15 μm^2 (FWHM) size and a Rayonix SX165 CCD detector (round active area of 165 mm diameter, frame size 2048 x 2048 pixels, 79 μm pixel size, dynamic range 16 bit). The energy used was 29.2 keV (λ = 0.4246Å) determined from the Sn absorption *K*-edge. The sample-detector distance and the beam centre position were calibrated using the Fit2D software (Hammersley *et al.*, 1994) from LaB_6 diffraction data measured at exactly the same conditions as the samples. Samples were mounted in a xyz stage with a vertical tilt axis (ϕ axis). The thin section was always faced to the detector as described in Rius *et al.* (2015). The transparency of the glass-substrate allows selecting the measurement point directly with a coaxial visualization system. The sample was mounted visually normal to the beam (sample-detector distance = 185.15mm). The exploration of the reciprocal space was performed by rotating the sample around the ϕ axis and performing small ϕ scans ($\Delta\phi$= 0.25º, time/frame= 0.5 s) which were stored as a sequence of 140 frames covering the ϕ range between -35.0 and +35.0º. Intensity extraction was performed with the single-crystal package XDS (Kabsch, 2000).

Table 2

3. Crystal structure refinement and discussion

The refinement was performed using SHELX (Sheldrick, 2008), using the data of Araki and Moore (1981) as starting model. Final graphics were generated with VESTA (Momma and Izumi, 2011). Miscellaneous information related to crystal data and structure refinement can be found in Table 2. Atomic coordinates and isotropic displacement parameters (DP) are listed in Table S1 and anisotropic DP are given in Table S2. Selected interatomic distances can be found in Table S3. Ionized scattering curves were used for all elements except for P. Site occupancies were assigned taking into account the aggregate scattering power of each site and the average <M-O> distance (M: metal). There is a good correspondence between the composition calculated from electron-microprobe analysis and crystal structure.

Figure 4

The topology of the minerals belonging to the fillowite group is already known, and the reader is referred to Moore (1989) and the publications mentioned in Table 1 (especially to that of Araki and Moore, 1981). The crystal structure ranks among the most complex structures known for phosphates. It can be rationalized as columns (*rods* in the terminology of Araki and Moore, 1981) of polyhedra located at the three fold rotation axis (Fig. 4). The cation sequence along a single column is M(1)-M(3)-Na(1)-Na(2)-M(4)-M(5)-M(2)-M(5)-M(4)-Na(2)-Na(1)-M(3)... Whereas the M(1) and M(2) octahedra are connected to the neighbouring polyhedra of the same column via bridging (PO_4) groups, sites M(3)-Na(1)-Na(2)-M(4)-M(5) define a block of five face-sharing polyhedra. These are octahedra except for the nine fold coordinated Na(2). The remaining four (PO_4) tetrahedra decorate these columns, defining a hexagonal motif when viewed down the *c* axis. These complex units are connected to other metals placed along the ternary screw axis at (x= 1/3, y= 1/3) [sequence is Ca(1)-M(9)-Na(3)-M(8)]. The two remaining metal atoms M(6) and M(7) at approximately (x= 1/3, y= 1/6) further link facing (PO_4) tetrahedra. Some characteristics of the chladniite structure reported in the present study appear in Table 3. The M(1) site at the unit cell origin is dominantly filled by Mn^{2+}; in contrast, in the very Mn-poor meteoritic chladniite it is occupied by Ca (Steele, 1994; McCoy *et al.* 1994). In this sense, terrestrial chladniite bears a closer resemblance to fillowite.

Table 3

As seen in other structures of this group, the coordination number of sites M(1) to M(11) (mainly occupied by Fe, Mn and Mg, with subordinate Ca) is 6 or 5. Sodium is also in octahedral coordination in site Na(1), but it is seven- or nine-fold coordinated in the other two sites [Na(2) and

Na(3)]. Ordering of divalent cations is also evident in (Mn,Fe)-rich chladniite. Some sites [most notably M(3), M(4) and M(5)] are almost exclusively occupied by Mg, which constitutes about 92-96% of the total cations in such positions. The highest site occupancy reached by (Fe+Mn) is about 87%. Based on the refined number of electrons and <M-O> distances, it is likely that a small fraction of Fe is trivalent, with $Fe^{3+}/(Fe^{2+}+Fe^{3+})$ around 0.14. Small quantities of Ca are disordered among some of the M sites, but this element is strongly concentrated in the Ca(1) position. It is interesting to note that fillowite, meteoritic chladniite and the sample studied here all display an occupancy of the Ca(1) position which is about 0.66 Ca:0.33 Na. Vacancies (≤ 15%) are present in some sites. An exception is site Na(1) which is only about half occupied.

These results clearly demonstrate the possibility of performing accurate crystal structure refinements from tts microdiffraction data thanks to the introduction of the very thin glass-substrate which makes accessible a larger portion of the weighted reciprocal space. In cases where the crystal structure model is unknown, the increased completeness of the intensity data set also facilitates the application of Patterson-function direct methods (Rius, 2014).

4. Comparison of chladniite from diverse occurrences

Based on chemical and textural evidences the paragenetic association beusite + chladniite has been interpreted as a replacement product of garnet during the magmatic stage, caused by destabilization of garnet due to phosphorus buildup in the magma (Colombo et al. 2012). The interested reader is referred to that publications for further details. A similar origin (reaction of biotite with P-enriched anatectic melt) is inferred for stornesite-(Y), another Mg-dominant member of the fillowite group (Grew et al. 2006).

As mentioned above, chladniite has been found before only in two meteorites: in the Carlton specimen (an IIICD iron meteorite, MacCoy et al. 1994) and in GRA 95209 (an acapulcoite-lodranite, Floss 1999). Whereas the type sample has very low contents of Mn and Fe (0.30 and 2.23 wt.%, as divalent oxides), chladniite from the GRA 95209 is richer in MnO (8.61 wt.% MnO) and especially Fe (14.4 wt.% FeO). The concentrations of these two elements are even higher in the Argentine sample (17.37 wt.% FeO, 14.42wt.% MnO), reflecting the pegmatitic environment. In the GRA 95209 meteorite, chladniite is also associated to graftonite (the Fe analogue of beusite). Floss (1999) suggests two possible hypothesis for the formation of chladniite: it could be either a replacement product of graftonite (which, in turn, originated by reaction of olivine and orthopyroxene with metallic iron containing dissolved P), or it could crystallize from the reaction of silicates (plagioclase and pyroxene) with metallic iron or schreibersite $[(Fe,Ni)_3P]$.

It is clear from published data (Table 1) that the composition is controlled by the geological environment of crystallization rather than by crystal chemical constraints. Another point worthy of note is that several occurrences [such as Loch Quoich area (Livingstone 1980), Larsemann Hills (Grew et al. 2006), Tablada I pegmatite (Colombo et al. 2012)], come from pegmatites or segregations which have no clear genetic link with granites, but rather seem to be related to partial melting during metamorphism and subsequent emplacement of such melts with minor chemical fractionation (such as that described by Shaw et al. 2016).

Acknowledgements: Thanks are due to Mr. Luis Gordón and Mr. Marc Puigcerver (Lab. de Preparació de Làmines Primes, Dpt. de Geologia, U. Autònoma de Barcelona) for their decisive contribution in the development of the technique, and to Dr. Jorge Sfragulla (U. Nac. de Córdoba) for help with the field work. The financial support of the Spanish 'Ministerio de Economía y Competitividad' (Projects 'NANOXRED': MAT2012-35247; MAT2015-67593-P and Severo Ochoa: SEV-2015-0496) is gratefully acknowledged. FC gratefully acknowledges CONICET for a stay at ICMAB. Thank are also due to the ALBA synchrotron (Barcelona, Spain) for beamtime (experiment Nr. 201521156) and to the 'Centres Científics i Tecnològics de la Universitat de Barcelona' for some EMP analyses .

References

Antenucci, D., Tarte, P. & Fransolet, A.-M. (1996): The synthetic phosphate $NaCaCdMg_2(PO_4)_3$: first experimental evidence of a reversible alluaudite-fillowite polymorphism. *Neues Jb. Miner. Monat.*, **171**, 289-296.

Araki, T. & Moore, P.B. (1981): Fillowite, $Na_2Ca(Mn,Fe^{2+})_7(PO_4)_6$: its crystal structure. *Am. Mineral.*, **66**, 827-842.

Brush, G.J. & Dana, E.S. (1879): On the Mineral Locality in Fairfield County, Connecticut, with the description of two additional new species. *Am. J. Sci. and Arts*, **17**, 359-368.

Colombo, F., Sfragulla, J. & González del Tánago, J. (2012): The garnet-phosphate buffer in peraluminous granitic magmas: a case study from pegmatites in the Pocho district, Córdoba, Argentina. *Can. Mineral.*, **50**, 1555-1571.

Domanskii, A.I., Smolin, Y.I., Shepelev, Y.F. & Majling, J. (1982): Determination of the crystal structure of triple magnesium calcium sodium orthophosphate $Mg_{21}Ca_4Na_4(PO_4)_{18}$. *Soviet Physics, Crystallography*, **27**, 535-537.

Fauth, F., Peral, I., Popescu, C. & Knapp, M. (2013): The new Material Science Powder Diffraction beamline at ALBA Synchrotron. *Powder Diffr*. **28**, S360-S370.

Fisher, D.J. (1965): Dickinsonites, fillowite and alluaudites. *Am. Mineral.*, **50**, 1647-1669.

Floss, C. (1999): Fe,Mg,Mn-bearing phosphates in the GRA 95209 meteorite: Occurrences and mineral chemistry. *Am. Mineral.*, **84**, 1354-1359.

Fransolet, A.-M., Fontan, F., Keller, P. & Antenucci, D. (1998): La serie johnsomervilleite-fillowite dans les asociacions de phosphates de pegmatites granitiques de l´Afrique centrale. *Can. Mineral.*, **36**, 355-366.

Grew, E.S., Armbruster, T., Medenbach, O., Yates, M.G. & Carson, C.J. (2006): Stornesite-(Y), $(Y,Ca)\square_2Na_6(Ca,Na)_8(Mg,Fe)_{43}(PO_4)_{36}$, the first terrestrial Mg-dominant member of the fillowite group, from granulite-facies paragneiss in the Larsemann Hills, Prydz Bay, East Antartica. *Am. Mineral.*, **91**, 1412-1424.

Hammersley,A.P, Svensson, S.O. & Thompson, A. (1994): Calibration and correction of distortions in 2D detector systems. *Nucl. Instr. Meth. A***346**, 312-321.

Hatert, F. & Fransolet, A.-M. (2003): Preliminary data on the crystal chemistry of synthetic fillowite-type phosphates. *Berichte der Deutschen Mineralogischen Gesellschaft, Beih. z. Eur. J. Mineral.*, **15**, 76.

Jerbi, H., Hidouri, M. & Amara, M.B. (2010): Synthesis and structural characterization of a new yttrium phosphate: $Na_{2.5}Y_{0.5}Mg_7(PO_4)_6$ with fillowite-type structure. *J. Rare Earth.*, **28**, 481-487.

Kabsch, W. (2000) XDS. *Acta Cryst. D* **66**, 125-132.

Keller, P., Hatert, F., Lissner, F., Schleid, T., & Fransolet, A.M. (2006): Hydrothermal synthesis and crystal structure of $Na(Na,Mn)_7Mn_{22}(P\ O_4)_{18}\cdot 0.5(H_2O)$, a new compound of fillowite structure type. *Eur. J. Mineral.*, **18**, 765-774.

Livingstone, A. (1980): Johnsomervilleite, a new transition-metal phosphate mineral from the Loch Quoich area, Scotland. *Mineral. Mag.*, **43**, 833-836.

McCoy, T.J., Steele, I.M., Keil, K., Leonard, B.F. & Endreß, M. (1994): Chladniite, $Na_2CaMg_7(PO_4)_6$: a new mineral from the Carlton (IIICD) iron meteorite. *Am. Mineral.*, **79**, 375-380.

Momma,K. & Izumi, F. (2011): VESTA 3 for three-dimensional visualization of crystal, volumetric and morphology data. *J. Appl. Crystallogr.*, **44**, 1272-1276.

Moore, P.B. (1989): Perception of structural complexity: Fillowite revisited and α-iron related. *Am. Mineral.*, **74**, 918-926.

Olsen, E. J., Kracher, A., Davis, A. M., Steele, I.M., Hutcheon, I.D. & Bunch, T.E. (1999): The phosphates of IIIAB iron meteorites. *Meteorit. Planet. Sci.*, **34**, 285-300.

Olsen, E. & Steele, I.M. (1997): Galileiite: A new meteoritic phosphate mineral. *Meteorit. Planet. Sci.*, **32**, 155-156.

Rius, J., Labrador, A., Crespi, A., Frontera, C., Vallcorba, O. & Melgarejo, J.C. (2011): Capabilities of through-the-substrate microdiffraction: Application of Patterson-function direct methods to synchrotron data from polished thin sections. *J. Synchrotron Radiat.* **18**, 891-898.

Rius, J. (2014): Application of Patterson-function direct methods to materials characterization. *IUCrJ*, **1**, 291-304.

Rius, J., Vallcorba, O., Frontera, C., Peral,I., Crespi, A. & Miravitlles, C. (2015): Application of synchrotron through-the-substrate microdiffraction to crystals in polished thin sections. *IUCrJ*, **2**, 452-463.

Shaw, R.A., Goodenough, K.M., Roberts, N.M.W., Horstwood, M.S.A., Chenery, S.R. and Gunn, A.G. (2016) Petrogenesis of rare-metal pegmatites in high-grade metamorphic terranes: A case study from the Lewisian Gneiss Complex of north-west Scotland. *Precambrian Res.*, **281**, 338-362.

Sheldrick, G.M. (2008): A short history of SHELX. *Acta Cryst. A***64**, 112-122.

Steele, I.A. (1994): Crystal structure of chladniite, $Na_2CaMg_7(PO_4)_6$, from Carlton (IIICD) meteorite. *Lunar and Planetary Science Conference XXV, Abstracts*, 1337-1338.

Zhesheng, M., Nicheng, S. & Danian, Y. (2005): Mineralogy and crystal structure determination of Mg-fillowite. *Sci. in China, Series D, Earth Sciences*, **48**, 635-646.

FIGURE CAPTIONS

Fig. 1. Cross-polarized photomicrograph of the studied polished thin section showing its general aspect and the various mineral constituents (beusite, garnet, chladniite and MgP). Analysis by tts-μXRD confirms that the greyish blue grains correspond to the complex phosphate chladniite, of which this is the first terrestrial occurrence. The phase labelled as MgP has not been identified yet.

Fig. 2. Two-stage procedure for preparing polished thin section on glass-substrates of 0.1mm: (A) The glass cover is fixed to the thick glass slide with soluble glue and to the rock slice with insoluble one; (B) Once the rock slice has been polished to the desired thickness, soluble glue is removed, so that the rock slice on the thin glass cover is ready for the diffraction experiment.

Fig. 3. Comparison of 2D frames of mineral beusite taken by tts-μXRD using the same experimental conditions except for the glass-substrate thicknesses (left: 1.5mm; right: 0.1mm). In the left image, it can be seen the high background around the origin due to the glass contribution which becomes even more evident when performing the circular integration (inset).

Fig. 4. Schematic view along *c* of selected features of the chladniite crystal structure: (bottom) metal site sequence with PO_4 tetrahedra along one rod; (top) arrangement of rods in the unit cell. Missing metal sites (omitted for clarity) are located between the rods.

Table 1. Mineral species belonging to the fillowite group. Site nomenclature after Araki & Moore (1981).

species	cation sites					selected references
	Na(1)	Na(2)+Ca	Na(3)	M(1)	M(2)-M(11)	
fillowite	Na_2	Ca_4Na_4	Na_6	Mn	Mn_{43}	1, 2
johnsomervilleite	$\square_2$	Ca_6Na_2	Na_6	Ca	Fe^{2+}_{43}	3*
chladniite§	Na_2	Ca_4Na_4	Na_6	Ca	Mg_{43}	4, 5, 6, this work
stornesite-(Y)	Na(3)	Ca_5Na_3	Na_6	Y	Mg_{43}	7
galileiite	Na_2	$Fe^{2+}_4Na_4$	Na_6	Fe^{2+}	Fe^{2+}_{43}	8*
unnamed phase	K_2	$Fe^{2+}_4Na_4$	K_6	Fe^{2+}	Fe^{2+}_{43}	9*

* Possible site occupancy assuming a fully ordered model. Structural refinements are not available.
§: stoichiometry of the phosphate described by McCoy *et al.* (1994). Other Ca- and Mg-dominant compositions are also possible (see Grew *et al.*, 2006). 1: Araki and Moore (1981), 2: Zhesheng *et al.* (2005), 3: Livingstone (1980), 4: McCoy *et al.* (1994), 5: Steele (1994), 6: Floss (1999), 7: Grew *et al.* (2006), 8: Olsen & Steele (1997), 9: Olsen *et al.* (1999).

Table 2. Crystal data and relevant parameters of the structure refinement of chladniite from tts microdiffraction data.

Empirical formula used for the refinement	$Na_{32.08}\ Ca_{16.52}\ Mg_{41.11}\ Fe_{45.83}Mn_{30.13}\ P_{108}\ O_{432}$
Formula weight (for the above composition)	16997.50
Temperature	293(2) K
Wavelength	0.42460 Å
Crystal system, space group	Trigonal, *R*-3 (#148)
Unit cell dimensions	$a = b = 15.0133(3)$ Å
	$c = 42.887(2)$ Å
Volume, Z	8371.6(5) $Å^3$, 3
Density (calculated)	3.372 Mg/m^3
Absorption coefficient	0.013 mm^{-1}
F(000)	8105
Crystal size	20 x 20 x 30 μm^3
Theta range for data collection	0.98 to 11.58°.
Index ranges	$-14 \le h \le 13, -13 \le k \le 14, -39 \le l \le 34$
Reflections collected	3719
Independent reflections	1617
R(int)	0.0502
Completeness to theta = 11.58°	97.1 %
Refinement method	Full-matrix least-squares on F^2
Data / restraints / parameters	1617 / 0 / 379
Goodness-of-fit on F^2	1.041
Final R indices [I>2σ(I)]	*R*1 = 0.0334, w*R*2 = 0.0812
R indices (all data)	*R*1 = 0.0358, w*R*2 = 0.0841
Largest diff. peak and hole	0.478 and -0.468 e.$Å^{-3}$

Table 3. Chladniite: Cation assignment to M sites based on refined scattering powers and mean bond lengths of corresponding sites.

Site	CN	Cation assignment								N	MAN	Scattering power [electrons]		Average bond length [Å]	
		Fe^{2+}	Fe^{3+}	Zn	Mn^{2+}	Mg	Ca	Na	□			refined	calculated	refined	calculated
M(1)	6	0.60			1.79	0.08	0.54			3	23.5	70.4	71.9	2.214	2.219
M(2)	6				0.33	2.40	0.27			3	14.2	42.6	42.5	2.121	2.123
M(3)	6	0.35				5.65				6	12.8	76.6	76.9	2.083	2.083
M(4)	6		0.48			5.52				6	13.0	78.3	78.7	2.054	2.074
M(5)	6					5.76	0.24			6	12.0	72.0	73.9	2.100	2.094
M(6)	5	9.04	1.71			7.25				18	20.3	366.2	366.4	2.103	2.103
M(7)	6			0.77	12.46	2.07	2.70			18	23.0	413.9	413.5	2.196	2.208
M(8)	6				6.66	10.08	1.26			18	17.4	312.6	312.7	2.149	2.145
M(9)	5	8.32	3.60		0.72	5.36				18	21.8	392.1	392.2	2.099	2.097
M(10)	6	3.56			12.24				2.20	18	22.1	398.5	398.7	2.221	1.913*
M(11)	5	12.82				5.18				18	21.9	395.1	395.4	2.123	2.123
Na(1)	6							2.87	3.13	6	5.3	31.6	31.6	2.457	1.245*
Na(2)	9				1.48			3.60	0.92	6	12.8	76.6	76.5	2.656	2.099*
Na(3)	7							17.60	0.40	18	10.7	193.3	193.6	2.534	2.543
Ca(1)	8						11.65	6.35		18	17.0	306.8	302.8	2.576	2.445
Σ (SC)		40.47		0.77	35.67	49.36	16.66	30.43				3200.8	3226.6		
Σ (EPM)		40.92		0.77	34.41	48.56	16.66	30.69							

CN: coordination number. N: site multiplicity. MAN: mean atomic number. *The marked discrepancy is due to the presence of vacancies, whose influence on the average bond length of these sites cannot be quantified. SC: single-crystal refinement. EPM: electron microprobe analysis.

FIGURE CAPTIONS

Fig. 1. Cross-polarized photomicrograph of the studied polished thin section showing its general aspect and the various mineral constituents (beusite, garnet, chladniite and MgP). Analysis by tts-μXRD confirms that the greyish blue grains correspond to the complex phosphate chladniite, of which this is the first terrestrial occurrence. The phase labelled as MgP has not been identified yet.

Fig. 2. Two-stage procedure for preparing polished thin section on glass-substrates of 0.1mm: (A) The glass cover is fixed to the thick glass slide with soluble glue and to the rock slice with insoluble one; (B) Once the rock slice has been polished to the desired thickness, soluble glue is removed, so that the rock slice on the thin glass cover is ready for the diffraction experiment.

Fig. 3. Comparison of 2D frames of mineral beusite taken by tts-μXRD using the same experimental conditions except for the glass-substrate thicknesses (left: 1.5mm; right: 0.1mm). In the left image, it can be seen the high background around the origin due to the glass contribution which becomes even more evident when performing the circular integration (inset).

Fig. 4. Coaxial experimental setup for monochromatic synchrotron tts microdiffraction (Rius *et al.*, 2015). The target point on the polished thin section is selected through a videocamera placed on the beam axis. During the measurement the thin section rotates around ϕ.

Fig. 5. Schematic view along *c* of selected features of the chladniite crystal structure: (bottom) metal site sequence with PO_4 tetrahedra along one rod; (top) arrangement of rods in the unit cell. Missing metal sites (omitted for clarity) are located between the rods.

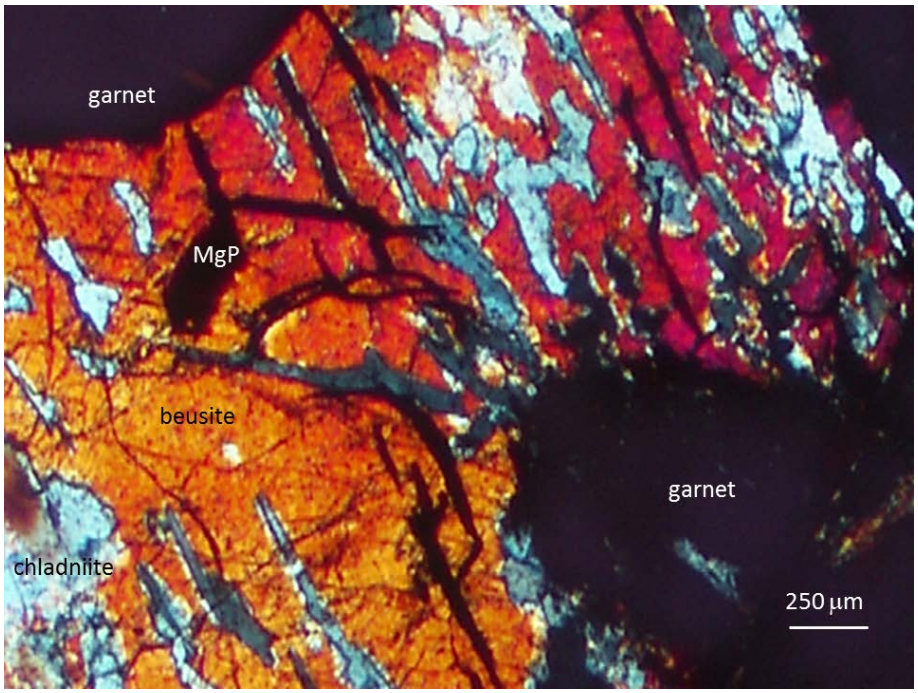
garnet
MgP
beusite
garnet
chladnite
250 µm

Fig. 1

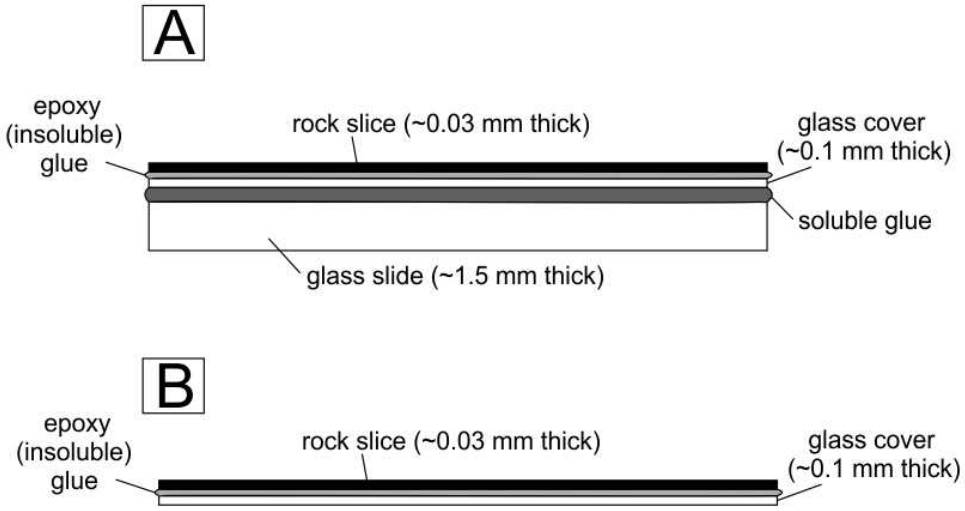
A
epoxy (insoluble) glue
rock slice (~0.03 mm thick)
glass cover (~0.1 mm thick)
soluble glue
glass slide (~1.5 mm thick)
B
epoxy (insoluble) glue
rock slice (~0.03 mm thick)
glass cover (~0.1 mm thick)

Fig.2

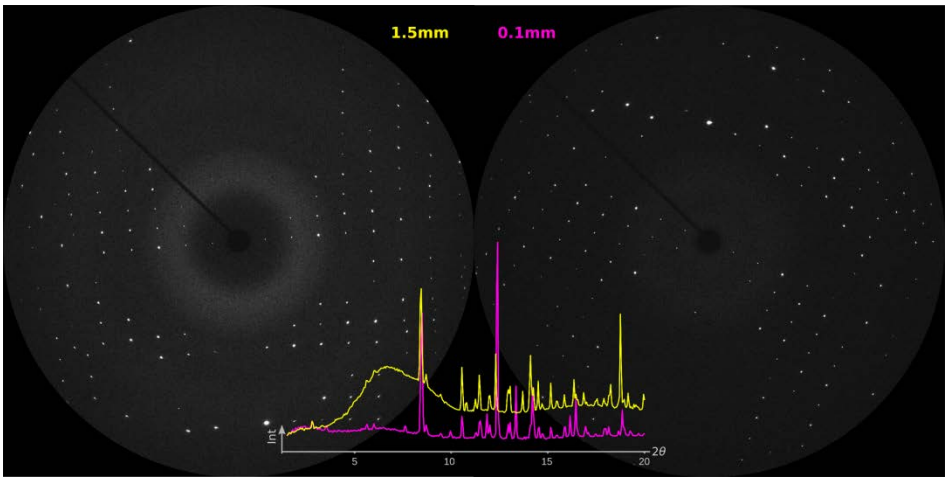
1.5mm
0.1mm
Int
5
10
15
20
2θ

Fig. 3

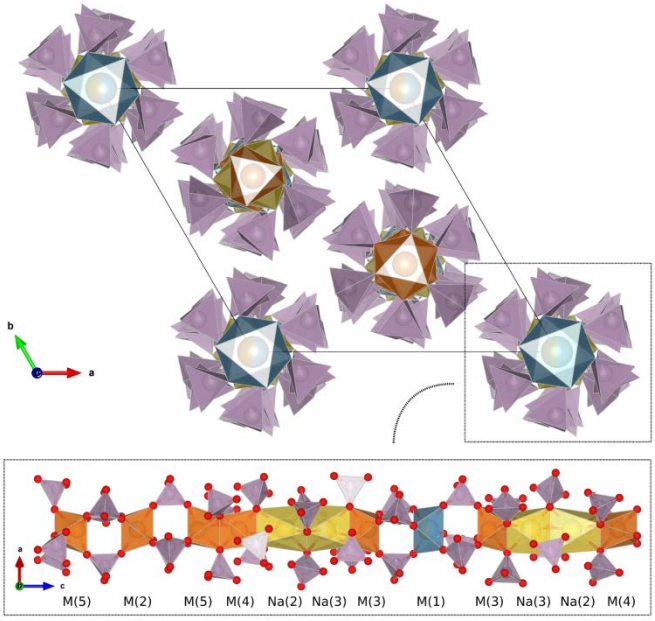
b
a
a
c
M(5)
M(2)
M(5)
M(4)
Na(2)
Na(3)
M(3)
M(1)
M(3)
Na(3)
Na(2)
M(4)

Fig. 4